


## Research

# Sustainable Pb(II) remediation: efficacy and selectivity of *Moringa Oleifera* composite nanofibers

Ronald Ngulube<sup>1</sup> · Nolwazi Nombona<sup>1</sup> · Letitia Pillay<sup>2</sup> 

Received: 21 February 2025 / Accepted: 10 April 2025

Published online: 06 October 2025

© The Author(s) 2025 

## Abstract

Nanofibers, with their unique properties are emerging as a promising solution for water remediation. Composite nanofibers often enhance basic aspects of remediation. We report the adsorption, selectivity and longevity of electrospun composite nanofibers synthesised from *Moringa oleifera* (*M. oleifera*) seed biomass incorporated into metal oxide nanoparticles (MONPs) and polyacrylonitrile (PAN) polymer blend. The composite fibres (PAN/*M. oleifera*/Fe<sub>3</sub>O<sub>4</sub>, PAN/*M. oleifera*/Fe<sub>3</sub>O<sub>4</sub>:Co and PAN/*M. oleifera*/Fe<sub>3</sub>O<sub>4</sub>:Mn) all showed an affinity for Pb(II) adsorption, however ionic strength and competing cations exerted varying inhibitory effects on Pb(II) adsorption. In naturally polluted wastewater, the composites demonstrated consistently high removal efficiencies (71.7—80.7%) and good selectivity (K) towards Pb(II) with values ranging from 10.3 to 30.4. Moreover, the composite demonstrated reusability and adsorption–desorption cycle stability, with adsorption capacities decreasing by only 13% for the composite with the best removal efficiency and selectivity (PAN/*M. oleifera*/Fe<sub>3</sub>O<sub>4</sub>:Mn) after five cycles. The cost assessment of PAN/*M. oleifera*/Fe<sub>3</sub>O<sub>4</sub>:Mn nanofiber adsorbent indicates its economic feasibility, making it a competitive alternative to conventional adsorbents. The prepared adsorbents have the potential to address challenges posed by heavy metal pollution in naturally polluted wastewater in an economical manner.

**Keywords** *Moringa oleifera* · Selective adsorption · Multi-ion system · Regeneration · Remediation · Wastewater

## 1 Introduction

High concentrations of heavy metals in wastewater present a serious threat to human health and ecological systems due to their toxicity and persistence in environment [1–5]. Lead (Pb), mercury (Hg) and arsenic (As) are specifically problematic since they have no natural physiological function. Lead is a particularly significant pollutant in the environment since it is a by-product in most industrial processes [6–9]. In naturally contaminated waters, Pb(II) ions are typically found alongside a mixture of various cations (e.g. Zn, Cd, Cu, Ni) as well as anions (e.g. SO<sub>4</sub>, Cl, NO<sub>3</sub>, PO<sub>4</sub> and CO<sub>3</sub>) [10]. The removal of Pb(II) ions from naturally contaminated waters can therefore present a complex challenge due to competitive adsorption from co-existing ions.

Numerous methods have been widely explored for removal of Pb(II) ions from wastewater, including chemical precipitation, ion-exchange, adsorption, membrane filtration, coagulation-flocculation, flotation, and electrochemical processes [10–15]. However, conventional methods such as precipitation and coagulation often require large quantities of chemical reagents leading to increased operational costs and the potential release of secondary pollutants into the environment

✉ Letitia Pillay, letitia.pillay@gmail.com | <sup>1</sup>Department of Chemistry, University of Pretoria, Pretoria 0002, South Africa. <sup>2</sup>Molecular Sciences Institute, School of Chemistry, University of the Witwatersrand, Johannesburg 2000, South Africa.



[16]. Furthermore, the sludge generated from these processes demands further treatment and disposal, posing serious environmental challenges [17]. Ion exchange resins, while effective in specific cases, tend to lose efficiency in the presence of competing ions due to their limited selectivity [18]. Similarly, membrane filtration technologies suffer from fouling caused by scaling and clogging, which increases both operational and maintenance costs [19]. Electrochemical treatments, such as electrocoagulation, are also hindered by their need for advanced equipment and high energy input, making them less viable for large-scale applications [20].

Given these limitations, adsorption has emerged as a widely favoured technique for the removal of lead from wastewater. This preference is largely due to its high efficiency, cost-effectiveness, operational simplicity and environmental sustainability. Unlike conventional methods, adsorption offers high selectivity for Pb(II) ions even in complex aqueous environments with multiple coexisting ions along with lower operational and energy costs, making it suitable for both large-scale and decentralized applications [21]. Moreover, adsorption processes typically operate under ambient conditions, involve minimal sludge generation and typically lower secondary pollution further enhancing their environmental appeal. However, despite these advantages, certain types of adsorbents, particularly bio-based adsorbents have been reported to suffer from limited regeneration and reduced reusability [22–24]. These factors can affect their long-term effectiveness and practicability especially in continuous or large-volume treatment systems. As such, ongoing research focuses on enhancing the durability and regeneration capacity of adsorbents to make adsorption not only high-performing but also a sustainable and scalable solution for heavy metal remediation.

The application of a broad range of adsorbent materials, including clay minerals, biochar, zeolites, biopolymer-derived adsorbents, industrial by-products, metal–organic frameworks (MOFs), covalent organic frameworks (COFs), and synthetic polymers, along with their modified forms, has been extensively explored for adsorption-based water remediation [25, 26]. Beyond the well-known advantages such as cost-effectiveness, high adsorption efficiency and environmental sustainability, these materials offer unique physicochemical properties that enhance their adsorption performance. For example, clay minerals and biochar not only offer large surface area and porosity but also exhibit ion exchange capabilities, making them effective at targeting a wide range of pollutants [27, 28]. Similarly, zeolites, with their crystalline structure provide unique cation-exchange properties and high thermal stability which enhances their reusability across multiple adsorption cycles even in harsh environments [29]. MOFs and COFs offer tunable porosity and high surface areas that allow for selective capture of contaminants in polluted waters [30]. Synthetic polymers can be tailored for specific adsorption applications, offering advantages in terms of mechanical strength, durability and flexibility. Their surface chemistry can be modified to enhance interaction with specific ions, making them adaptable for diverse water qualities [31]. The versatility of these adsorbents lies in their regeneration and reusability which reduces the need for continuous replacement and minimizes waste [32–34]. Moreover, many of these materials offer additional functional groups such as carboxyl, hydroxyl, and amine groups that enable the selective binding of metal ions, providing an additional layer of specificity and efficiency in adsorption process [35]. These materials contribute significantly to advancing sustainable and efficient wastewater treatment solutions by reducing contaminant levels, minimizing chemical use and lowering secondary pollution [36].

Recently, there has been growing interest in utilizing plant-derived materials, such as rice husks, wheat shells, cereal chaff, raw dust, and pine bark, for the development of multifunctional adsorbents. These biomass-based materials are particularly attractive due to their wide availability, renewability, biodegradability, non-toxicity and biocompatibility, all of which contribute to a reduced environmental footprint [37–39]. In addition, the diverse functional groups present in these materials—such as phosphate, hydroxyl, carboxyl, amine, and amide—enhance their surface adsorption properties by enabling selective binding of multiple coexisting metal ions based on individual functional group affinities [24, 31]. This multifunctionality is expected to reduce competitive adsorption effects, improving overall adsorption efficiency in complex wastewater matrices. However, despite their numerous advantages, the use of pure bio-based fibers as adsorbents presents certain limitations. Natural polymer adsorbents are prone to structural degradation over time, which affects their stability and reusability in water treatment applications [32]. The poor regeneration ability of these materials restricts their long-term applicability.

The utilisation of nano-based substrates incorporating plant-based biomass has garnered considerable interest in the adsorption of heavy metal ions. Electrospun composite nanofibers, serving as polymeric templates, represent an excellent substrate due to their ability to incorporate a diverse range of materials at the nanoscale. The resulting composites not only retain the inherent physicochemical properties but also exhibit improved stability and processability due to the synergistic functions from individual materials [33]. This has effectively been reported for a number of different composites; clay-chitosan, (CS) nanofibers [33], CS/cellulose nanofiber-Fe(III) composite nanofibers [34] and amyloid fibril CsgA

proteins with Fe<sub>3</sub>O<sub>4</sub> nanoparticles [35]. These studies showed enhanced adsorption, selectivity and reusability for Ni(II), Cu(II), Cr(VI) and Pb(II) from contaminated water sources.

In the pursuit of developing multifunctional and sustainable adsorbents, this study explores a composite material combining *Moringa oleifera* (*M. oleifera*) biomass, metal oxide nanoparticles and polyacrylonitrile nanofibers. For the removal of Pb (II) ions from contaminated water. The innovation lies in the strategic integration of natural, inorganic and synthetic constituents, each contributing distinct yet complimentary adsorption functionalities. *M. oleifera* is a widely available, biodegradable and non-toxic plant biomass rich in functional groups that have high affinity for heavy metal ions [36]. Its inclusion introduces eco-friendly and cost-effective adsorption capabilities, enhancing the materials sustainability. To improve the structural and mechanical stability of the adsorbent, *M. oleifera* was embedded in a PAN polymer matrix, known for its excellent electrospinnability, mechanical durability and chemical resistance. In our previous work the PAN/*M. oleifera*/MONP nanofiber composites demonstrated good adsorption capacities [37]. PAN forms a stable and flexible fibrous network, offering a robust platform for adsorbent fabrication [40]. To further enhance the composite, metal oxide nanoparticles are added which contribute greatly to the adsorption efficiency due to their high surface reactivity, large specific surface area and their ability to facilitate rapid ion exchange. The presence of MONPs improves heavy metal uptake and helps overcome limitations commonly associated with bio-based adsorbents such as poor reusability. The composite system exhibits synergistic properties that enable efficient Pb(II) ion adsorption in simple and complex wastewater matrices.

The integration of *M. oleifera* biomass and metal oxide nanoparticles into a PAN nanofiber matrix will result in a composite adsorbent with enhanced selectivity, adsorption capacity, and reusability for Pb(II) removal from simple and complex wastewater systems. The synergistic interactions of the components are expected to overcome the limitations of individual components offering a sustainable and efficient solution for heavy metal remediation.

## 2 Materials and methods

Iron chloride (FeCl<sub>3</sub>), iron sulfate heptahydrate (FeSO<sub>4</sub>·7H<sub>2</sub>O), manganese sulfate (MnSO<sub>4</sub>·H<sub>2</sub>O), cobalt sulfate (CoSO<sub>4</sub>), potassium permanganate (KMnO<sub>4</sub>), sodium hydroxide (NaOH), hydrochloric acid (HCl), polyacrylonitrile (PAN) with average MW 150000, N, N-dimethylformamide (DMF), sodium chloride (NaCl), lead nitrate (Pb(NO<sub>3</sub>)<sub>2</sub>, 98%), nitric acid (HNO<sub>3</sub>), lead chloride (PbCl<sub>2</sub>), copper chloride (CuCl<sub>2</sub>), zinc chloride (ZnCl<sub>2</sub>), cobalt chloride (CoCl<sub>2</sub>), sodium sulphate (Na<sub>2</sub>SO<sub>4</sub>), sodium carbonate (Na<sub>2</sub>CO<sub>3</sub>) and ethanol were of analytical grade and purchased from Sigma-Aldrich. *M. oleifera* seeds were purchased from Umoyo Natural Health Store, Zambia.

### 2.1 Synthesis of metal oxide nanoparticles and *M. oleifera*-based nanofibers

Fe<sub>3</sub>O<sub>4</sub>, Co and Mn-doped Fe<sub>3</sub>O<sub>4</sub> nanoparticles were synthesized using chemical co-precipitation methods as described in our previous study [37]. The synthesis involved aqueous reactions of Fe<sup>3+</sup>/Fe<sup>2+</sup> salts with NaOH under controlled conditions. For the Co-doped samples, Co<sup>2+</sup> was introduced into the precursor mixture followed by hydrothermal treatment. The synthesis of Mn-doped Fe<sub>3</sub>O<sub>4</sub> followed a modified co-precipitation method which involved MnSO<sub>4</sub> and KMnO<sub>4</sub> as oxidising agents, with sequential mixing, room temperature stirring and final drying.

The extraction of *M. oleifera* seed proteins and fabrication of PAN/*M. oleifera*/MONPs nanofibers were carried out using methods established in our previous work [37]. The extract was prepared through ethanol-based defatting followed by saline extraction and freeze-drying. The nanofibers were synthesized by blending PAN with *M. oleifera* extract and metal oxide nanoparticles in DMF, followed by stirring, sonication and electrospinning under optimized conditions.

### 2.2 Instrumentation

The electrospinning setup was equipped with a voltage power supply (JDF-1, Beijing, China) and a syringe driver (789100C, Cole-Parmer, Vernon Hills, IL, USA). For morphological analysis, a Zeiss Ultra-Plus 55 Field-Emission Scanning Electron Microscope (FE-SEM) with an energy-dispersive X-ray spectrometer (EDS) from Oxford Link-ISIS-300 (Germany) was used. Adsorption experiments were conducted using a JEIO Mechanical Shaker model 6 K-300, operating at 100 rpm. Metal ion concentrations were measured using the Inductively Coupled Plasma Optical Emission Spectrometer (ICP-OES 5110, Agilent, USA). Each sample was analysed in triplicate.

### 2.3 Effect of ionic strength

The influence of ionic strength on competitive adsorption was assessed using a range (0, 0.005, 0.05, and 0.5 mol/L) of NaCl solutions encompassing values found in fresh water (~0.002 mol/L) to almost seawater (0.6 mol/L). Individual ionic solutions were added to 20 mL of 5 mg/L Pb(II) solutions containing a 1 mg sheet of the PAN/*M. oleifera*/MONPs nanofibre mats. The solution pH was maintained at optimal value of 8.0 [37]. The contents were agitated in a rotary shaker for 8 h and subsequently centrifuged. The supernatants collected were analysed for Pb(II) ions. Equilibrium adsorption capacity ( $q_e$ ) was calculated using Eq. (1) [39–44].

$$q_e = \frac{(C_i - C_e) \times V}{m} \quad (1)$$

where  $C_i$  and  $C_e$  are the initial and equilibrium metal concentrations respectively (mg/L);  $V$  is the volume of the solution (L), and  $m$  is the amount of composite fibre mat used (g).

### 2.4 Effect of cations in binary systems

Co(II), Cu(II) and Zn(II) were selected to test the selectivity of the synthesised nanofibers towards Pb(II) ions. Solutions (20 mL) containing 5 mg/L Pb(II) combined with either 2.5 mg/L or 5 mg/L of each individual metal were prepared. All solutions were adjusted to optimal pH (8.0), added to test tubes containing the PAN/*M. oleifera*/MONPs nanofibre mat, equilibrated for 8 h and centrifuged. The supernatant was analysed for Pb(II), Zn(II), Cu(II) and Co(II). The % removal efficiency (RE), distribution coefficient ( $K_d$  in L/g) and selectivity ( $K$ ) values were calculated using Eqs. (1), (2) and (3) respectively [3].

$$RE = \frac{(C_i - C_e)}{C_i} \times 100 \quad (2)$$

$$K_d = \frac{q_e}{C_e} \quad (3)$$

$$K = \frac{K_{d(\text{Pb(II)ions}}}{K_{d(\text{co-existing ions})}} \quad (4)$$

Higher  $K$  values represent a stronger affinity between the target ion Pb(II), and the adsorbents.

### 2.5 Effect of competing ions in multi-ion systems

The synthesised composite nanofiber mat (1 mg) was immersed in 20 mL of natural water samples. The samples were equilibrated for 8 h, followed by centrifugation. The supernatants were then analysed for Pb(II), Zn(II), Co(II), and Cu(II).

#### 2.5.1 Sample area

Natural water samples were collected from Kabwe in central Zambia, a region severely impacted by historical mining activities that have caused extensive water quality degradation [45]. The area is particularly known for elevated Pb(II) contamination [46]. Recent studies report that 74.9% of Kabwe's residents exhibit blood lead levels (BLLs) exceeding 5 µg/dL, a threshold associated with serious health risks, especially in children [47, 48]. Additionally, elevated Pb levels have also been detected in livestock and crops [49], intensifying the risk of lead exposure through the food chain. This presents a substantial health risk to local populations. Water samples analysed from the Kabwe Mine Drainage Canal revealed extensive contamination with lead (Pb), cadmium (Cd), zinc (Zn), copper (Cu), and cobalt (Co). Over time, this canal has become a persistent source of heavy metal pollution endangering aquatic ecosystems, agricultural productivity and public health [50]. The findings highlight the needs for sustainable and effective remediation strategies to mitigate the ongoing environmental health crisis posed by heavy metals pollution in Kabwe.

**Fig. 1** SEM images of **a** PAN/*M. oleifera*/Fe<sub>3</sub>O<sub>4</sub> **b** PAN/*M. oleifera*/Fe<sub>3</sub>O<sub>4</sub>:Co **c** PAN/*M. oleifera*/Fe<sub>3</sub>O<sub>4</sub>:Mn. [37]

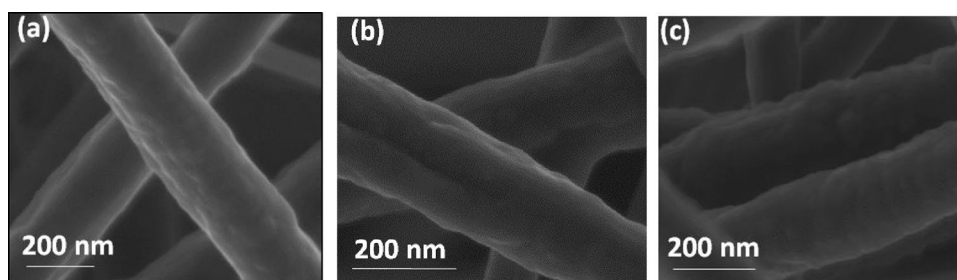
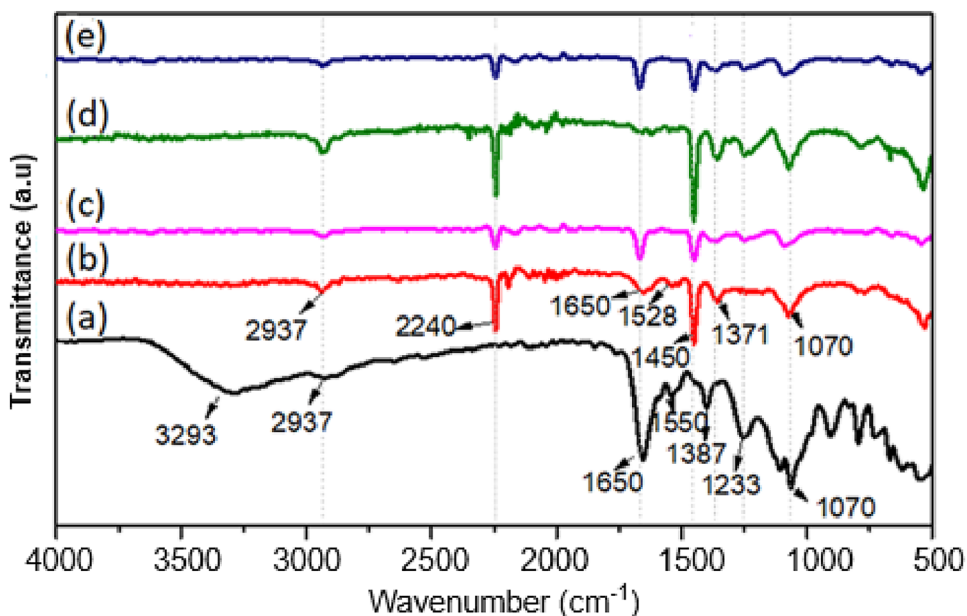


**Fig. 2** FTIR spectra of **a** *M. oleifera* powder **b** PAN powder **c** PAN/*M. oleifera*/Fe<sub>3</sub>O<sub>4</sub> **d** PAN/*M. oleifera*/Fe<sub>3</sub>O<sub>4</sub>:Mn **e** PAN/*M. oleifera*/Fe<sub>3</sub>O<sub>4</sub>:Co nanofibers. [37]



## 2.6 Regeneration experiments in multi-ion systems

The regeneration performance was carried out on PAN/*M. oleifera*/MONPs fibre mats, previously used for adsorption in a mg/L Pb(II) solutions. The mat was immersed in 0.1 M HNO<sub>3</sub> acid and agitated at 150 rpm for 8 h. The nanofibre mat was separated from the solutions by filtration, washed several times with deionised water to remove the residual solution, and then dried at 60 °C for 12 h. The mat underwent adsorption with 5 mg/L Pb(II) for 8 h. The adsorption–desorption cycle of the regenerated nanofibre adsorbent was repeated five times. The filtrate at each stage was collected and analysed for Pb(II) via ICP-MS.

## 3 Results and discussion

### 3.1 Structural and functional characterization of the composite nanofiber

The surface morphology of PAN/*M. oleifera*/MONP nanofibers, including the integration of metal oxide nanoparticles, was characterized in our previous work [37]. The SEM analysis (Fig. 1) revealed a rough and uneven surface, indicating successful nanoparticle embedding. This surface structure contributes to improved adsorption performance by increasing surface area and enhancing interactions with Pb(II) ions [51–54].

FTIR spectral analysis (Fig. 2) of the composite nanofiber was conducted in the previous study to identify key functional groups [37]. The spectra confirmed the presence of typical PAN functional groups, including the nitrile (C≡N) stretch, as well as bands corresponding to *M. oleifera* seed extract components such as O–H (3293 cm<sup>-1</sup>), C–H (2937 cm<sup>-1</sup>), C=O (1650 cm<sup>-1</sup>), and C–O (1070 cm<sup>-1</sup>) stretching. These features indicate successful incorporation of the extract into the

nanofiber matrix and suggest intermolecular interactions between PAN, MONPs, and *M. oleifera* constituents [55–57]. Additional characterization data supporting the structural integrity and composite formation including XRD, and BET analysis can be found in previously work [37].

### 3.2 Ionic strength

The influence of ionic strength was investigated to assess its effect on the Pb(II) adsorption performance. All three prepared composite nanofibers showed a similar adsorption trend when exposed to solutions of differing ionic strengths (Fig. 3). The adsorption capacities at both 0.005 M and 0.05 M NaCl were not significantly different to that of the control. The 0.5 M solution resulted in a decrease in adsorption capacities by approximately 15%. The Mn-containing composite fibre showed the highest adsorption capacity (114 – 145 mg/g) and follows the reported trends of Mn-based nanomaterials' ability to alleviate/tolerate salt stresses [57].

The ionic strength concentration range used for testing the PAN/*M. oleifera*/Fe<sub>3</sub>O<sub>4</sub> doped fibres were selected to encompass a range of natural water samples; surface water (0.001–0.005 M), potable/groundwater (0.01 – 0.02 M) and estuarine water (up to 0.7 M). It is notable that the composite fibres showed limited change in adsorption capacity in water mimicking surface and potable water. At the higher ionic strength, Na<sup>+</sup> and Cl<sup>-</sup> likely to cause steric hindrance of Pb(II) uptake, competing for surface adsorption sites on the nanofibers leading to reduced adsorption capacities. Similar results on inhibiting performance of Na<sup>+</sup> and Cl<sup>-</sup> on Pb(II) adsorption have been reported [58, 59].

The changes in adsorption capacity for composite nanofibers subjected to parameters most likely to be encountered in natural systems, is an important aspect of evaluating their efficacy. Ionic strength and how other cations interact are two of the most common parameters which render composite nanofibers ineffective for remediation.

### 3.3 Competitive adsorption: binary metal systems

Lab -simulated solutions containing only Pb(II) exhibited significant removal efficiency values (Table 1) with the Co-containing nanofiber (92.2%) and Mn-containing nanofiber (95.6%) compared to the non-doped Fe<sub>3</sub>O<sub>4</sub> nanofiber (86.4%).

#### 3.3.1 Zn(II)/Pb(II) binary solutions

The addition of Zn(II) to Pb(II) solutions resulted in a decrease (5–9%) in the overall removal efficiency of Pb(II) from solution for each of the nanofibers. The Co-containing nanofiber adsorbents were most affected by the addition of Zn(II) with a decrease in removal efficiency of 9%. There did not appear to be a significant difference in having different Zn(II) concentrations on the Pb(II) removal efficiency for the non-doped Fe<sub>3</sub>O<sub>4</sub> and Co-containing nanofiber, however, the 2:1 Pb(II)/Zn(II) solution showed significantly less removal efficiency (87%) than the 1:1 ratio (93%). The adsorption of Zn(II) in all three nanofiber adsorbents was consistent ranging from 12–16%.

Fig. 3 Effect of ionic strength on the adsorption of Pb(II)

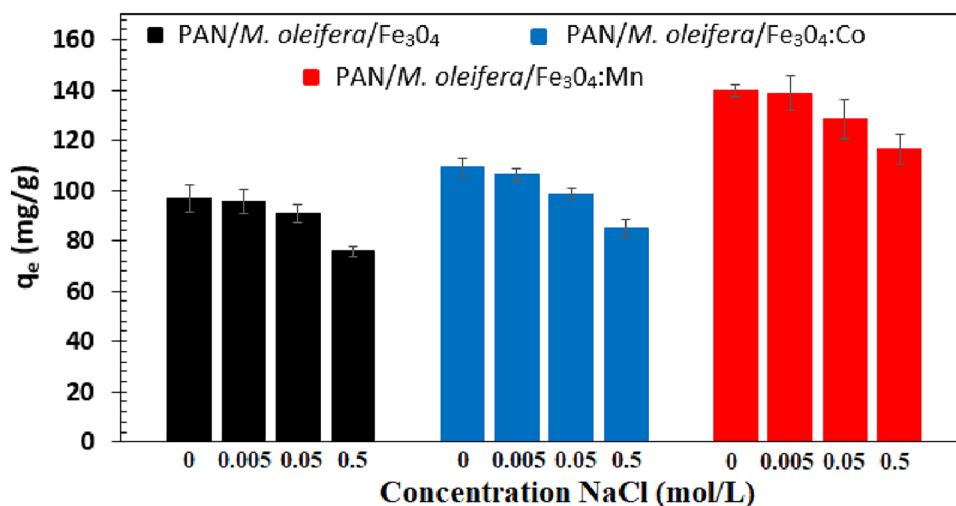


**Table 1** Effect of competing cations on Pb(II) adsorption in binary systems

Metal ion	Ratio in solution	PAN/ <i>M. oleifera</i> /Fe <sub>3</sub> O <sub>4</sub>		PAN/ <i>M. oleifera</i> /Fe <sub>3</sub> O <sub>4</sub> :Co		PAN/ <i>M. oleifera</i> /Fe <sub>3</sub> O <sub>4</sub> :Mn	
		Average RE (%)	Standard Deviation	Average RE (%)	Standard Deviation	Average RE (%)	Standard Deviation
Pb(II)	Single	86.43	0.11	92.22	0.65	95.58	0.42
Pb(II)	2:1	78.97	2.32	84.60	0.89	86.59	0.93
Zn(II)		12.00	2.39	13.00	1.43	12.88	0.91
Pb(II)	1:1	77.93	2.92	81.40	2.14	93.32	0.24
Zn(II)		13.36	1.66	15.78	1.72	16.33	1.58
Pb(II)	2:1	71.22	3.63	81.36	0.81	86.59	0.93
Cu(II)		11.26	1.65	10.75	2.46	11.45	0.93
Pb(II)	1:1	71.22	3.63	77.23	1.78	80.35	0.88
Cu(II)		8.55	2.69	9.42	2.28	8.38	2.33
Pb(II)	2:1	78.97	1.56	81.70	0.40	93.51	0.15
Co(II)		19.20	2.77	16.10	2.37	20.92	4.65
Pb(II)	1:1	73.69	2.34	83.85	1.17	82.98	1.24
Co(II)		14.53	1.25	18.73	3.22	16.39	2.77

### 3.3.2 Pb(II)/Cu(II) binary solutions

The significant decrease in removal efficiency of Pb(II) from the solutions containing Cu(II) was noted (12–15%). The non-doped Fe<sub>3</sub>O<sub>4</sub> fibres were once again most affected by the binary solutions. Both the Co and Mn-containing fibres showed further decreases in removal efficiency when the Cu(II) ratio was increased. Despite these variations, the Cu(II) removal efficiency for all fibres remained between 8–11%. The 1:1 ratio results in lower adsorption than the 2:1 Pb(II)/Cu(II) solution.

### 3.3.3 Pb(II)/Co(II) binary solution

The Pb(II)/Co(II) solutions followed the trend of decreasing removal efficiency. Co(II) adsorption for all the nanofibers was higher than for Zn(II) and Cu(II), ranging from 15 to 21%. The Mn-containing nanofiber adsorbents showed the most marked decrease when the ratios between metals was 1:1.

### 3.3.4 Binary solution metal removal efficiency

Controlled lab-simulated solutions provide a simplified environment for examining the physicochemical factors that influence adsorption, particularly in competitive adsorption studies. The experimental results demonstrated that competing cations, namely Cu(II), Zn(II), and Co(II), exhibited varying degrees of inhibition on Pb(II) adsorption. Among them, Cu(II) exerted the most substantial inhibitory effect, followed by Zn(II) and Co(II) in binary adsorption systems. Interestingly, despite its stronger competitive influence, Cu(II) had the lowest removal efficiency compared to Zn(II) and Co(II).

The extent of this inhibitory effect was found to be dependent on multiple factors, including the nature of the adsorbent, the initial Pb(II) concentration and the concentration of competing cations. A higher concentration of competing ions increases the number of species vying for the limited adsorption sites, thereby intensifying competition and potentially reducing Pb(II) adsorption efficiency [60, 61]. In binary systems, the shared adsorption sites result in a decrease in Pb(II) uptake, making it less likely to achieve the high removal efficiencies observed in single-ion systems. This trend is consistent with previous studies on heavy metal adsorption using composite nanofibers [62, 63].

The preferential adsorption of one metal ion over another in competitive systems is dictated by a complex interplay of factors, including the chemical affinity of the ions, their ionic radii, hydration energy, charge density, and the specific properties of the adsorbent material. Ions with lower hydration energy and larger ionic radii tend to adsorb more readily due to their increased ability to interact with available surface functional groups. Moreover, the structural and electronic properties of the adsorbent influence metal ion coordination, affecting the selectivity and efficiency of adsorption. These findings align with prior research on competitive adsorption mechanisms in nanostructured adsorbents [64, 65].

### 3.4 Competitive adsorption: naturally polluted water

The adsorption studies in samples from the natural environment were evaluated to further understand the interference of various coexisting ions present in the water on Pb(II) adsorption (Table 2). The initial analysis of Pb(II), Zn(II), Cu(II) and Co(II) in the samples collected from the effluent from Kabwe mine drainage canal showed elevated levels of all contaminants ranging from 3.9 – 12 mg/L. Adsorption experiments were conducted at both the natural effluent solution (pH 5.6) and the optimized value of pH 8.0. Both pH values showed robust uptake of all the metals, particularly with Pb(II).

Pb(II) removal efficiencies from the samples at the natural effluent pH of 5.6 were 63.9% (non-doped Fe<sub>3</sub>O<sub>4</sub>), 71.5% (Co-containing nanofibre) and 74.1% (Mn-containing nanofibre). While at optimal solution pH of 8.0, the removal efficiencies obtained were 71.7% (non-doped Fe<sub>3</sub>O<sub>4</sub>), 77.0% (Co-containing nanofibre) and 80.7% (Mn-containing nanofibre). The finding aligns with previous research, which noted that at high pH levels (above the point of zero charge pH<sub>PZC</sub>), the negatively charged surface of the adsorbents promotes the adsorption of positively charged metal ions through electrostatic attraction [37]. Efficiency for Pb(II) removal was improved between 5 – 8% at the optimised pH of 8.0. Additionally, improvements in the removal efficiencies were also noted for all the other metals ions at the increased pH values. However, adjusting pH at an industrial scale can be challenging due to cost and practicality concerns. A greener alternative could be to integrate alkaline industrial waste to increase pH and this may provide a cost-effective and sustainable approach without excessive reagent consumption [66].

The adsorption of Co(II), Zn(II) and Cu(II) in the natural solution was significantly lower than the laboratory prepared solutions (binary solutions) demonstrating that the complexity of the sample matrix may have affected the optimum adsorption of Pb(II) ions. Given the similarity in concentration of Pb(II), Zn(II) and Co(II) in the effluent sample, there is a clear indication of selectivity with Pb(II) effectively separated from polluted water comprising multi-ions. The decrease in removal efficiency of Pb(II) ion by the prepared adsorbents in multi-heavy metal ions solution can be attributed to competitive adsorption and less availability of binding sites on the surface of the adsorbents [62, 67, 68].

The removal efficiency of the four analyzed heavy metal ions followed the order: Pb(II) > Co(II) > Zn(II) > Cu(II). The high selectivity of the synthesized nanofibers towards Pb(II) ions can be attributed to several physicochemical properties, including ionic radius, electronegativity, hydration energy and functional group interactions. Pb(II) exhibited the highest adsorption efficiency, which can be primarily attributed to its larger ionic radius (0.118 nm) compared to Zn(II) (0.075 nm), Co(II) (0.074 nm), and Cu(II) (0.073 nm). A larger ionic radius generally results in a more diffuse electron cloud, which enhances electrostatic attraction between Pb(II) ions and the functional groups present on the nanofiber surface. The increased size also facilitates easier access to available adsorption sites, thereby improving coordination with active functional groups, which play a key role in Pb(II) ion binding [69].

Adsorption selectivity is controlled by a combination of electronegativity, hydration energy, and functional group interactions. The moderate electronegativity of Pb (2.33), compared to both Cu (2.00) and Zn (1.65) facilitates effective bonding with the adsorbent's functional groups [70]. Pb(II)'s lower hydration energy (-1481 kJ/mol) compared to Cu(II) (-2100 kJ/mol), Zn(II) (-2045 kJ/mol), and Co(II) (-1996 kJ/mol) allows for easier dehydration, making it more readily available for adsorption [71]. Conversely, the higher hydration energies of Cu(II) and Zn(II) hinder their interaction with the adsorbent due to stronger solvation. Finally, the interaction between metal ions and the oxygen- and nitrogen-containing

**Table 2** Effect of competing cations on Pb(II) adsorption in multi-ion system

		Initial concentration (mg/L)	PAN/M. oleifera/ Fe <sub>3</sub> O <sub>4</sub>		PAN/M. oleifera/ Fe <sub>3</sub> O <sub>4</sub> :Co		PAN/M. oleifera/ Fe <sub>3</sub> O <sub>4</sub> :Mn	
			pH 5.6	pH 8	pH 5.6	pH 8	pH 5.6	pH 8
Natural	Pb	12.05	63.91%	71.73%	71.51%	77.01%	74.08%	80.69%
	Zn	10.46	26.77%	30.02%	14.01%	15.92%	11.02%	12.91%
	Cu	3.89	10.86%	14.54%	5.71%	7.78%	6.21%	9.22%
	Co	8.28	15.73%	20.02%	23.2%	23.2%	16.66%	19.17%
Lab	Pb	5.00		86.43%		92.22%		95.58%
	Pb binary	Average 1:1 and 1:2 ratios		75.33%		81.69%		87.22%
	Zn binary			12.68%		14.39%		14.61%
	Cu binary			9.90%		10.09%		9.91%
	Co binary			16.86%		17.41%		18.65%

functional groups in the PAN/*M. oleifera*/MONP composite nanofibers is significant. Pb(II), with its larger ionic radius and favourable electronegativity, forms stronger surface complexes compared to smaller, highly charged ions like Cu(II), which may prefer complexation with ligands in solution [72]. This interplay underscores the potential of these nanofibers for selectively removing Pb(II) from contaminated water, making them promising for heavy metal remediation.

The interaction of the target metal ion (Pb(II)) in the presence of competing ions with the prepared adsorbents can be further evaluated by the  $K_d$  and  $K$  values (Table 3). The  $K_d$  values represent an important aspect of the adsorbent performance with values over 10.0 L/g generally indicating a good adsorbent [72–74]. In this study, all three nanofibers were deemed to be good adsorbents with the Mn-composite being the most notable (50 L/g). In addition, the  $K$  values ranged between 10.3 – 19.0, 11.0 – 18.8 and 30.2 – 30.4 for non-doped Fe<sub>3</sub>O<sub>4</sub>, Co-containing and Mn-containing nanofibers, respectively. These results suggest that the synthesised adsorbents had superior selectivity towards Pb(II) ions in multi-ion systems with Mn-containing nanofiber adsorbent recording the highest affinity.

### 3.5 Regeneration

The adsorption–desorption cycles show Pb(II) removal efficiencies gradually reducing with re-use (Fig. 4) for all three nanofiber adsorbents. The decline in removal efficiency was most evident in the non-doped Fe<sub>3</sub>O<sub>4</sub> fibres. After the third regeneration cycle, a plateau is noted for all fibres. Overall decreases of 10.2%, 13.5% and 18% for the Mn-, Co- and non-doped Fe<sub>3</sub>O<sub>4</sub> fibres were recorded, respectively. In terms of adsorption capacity, this decline corresponded to a reduction from 139 to 121 mg/g for Mn-doped Fe<sub>3</sub>O<sub>4</sub> fibers, 116 to 83 mg/g for Co-doped Fe<sub>3</sub>O<sub>4</sub> fibers, and 98 to 77 mg/g for the un-doped Fe<sub>3</sub>O<sub>4</sub> fibers. All the three composite fibres showed slight reduction (10–18% loss) in Pb(II) recovery after five regeneration cycles reaching a plateau after the third cycle. This indicates that the materials maintained considerable integrity and demonstrated favourable reusability and cycle stability. Consequently, these characteristics would make the materials economically feasible adsorbents for removing Pb(II) in complex water systems.

SEM images of the nanofiber adsorbents before and after five adsorption–desorption cycles (Fig. 5) confirm that the core nanofiber structure remains largely intact, with only minor surface modifications. The relatively stable morphology, along with sustained Pb(II) ion removal efficiency after five cycles, suggests that the composite nanofiber remained structurally viable for reuse. While acid exposure is known to induce protonation or partial dissolution of functional groups, which may present as slight surface changes [73–75], the extent of degradation observed was minimal. The oxide nanoparticles used in this study exhibit good acid resistance at moderate concentrations (0.1 M HNO<sub>3</sub>), making significant nanoparticle detachment and leaching unlikely under the experimental conditions. If structural compromise or nanoparticle loss had occurred, a noticeable drop in adsorption performance would be expected, which was not observed. These findings suggest that the nanofibers demonstrate promising short-midterm stability and are potentially suitable for extended application in cyclic adsorption processes though further studies over more cycles would be beneficial to fully validate long-term operational stability.

Nevertheless, the use of nitric acid for desorbing adsorbents raises environmental concerns, particularly regarding its disposal. While 0.1 M HNO<sub>3</sub> presents minimal environmental risk in this study, improper disposal can lead to wastewater acidification. Despite these concerns, HNO<sub>3</sub> remains a widely used eluent in metal adsorption studies due to its strong

**Table 3** The values of  $K_d$  and  $K$  of coexisting ions

Adsorbent	Co-existing ions	$K_d$ (L/g)	$K$
PAN/ <i>M. oleifera</i> /Fe <sub>3</sub> O <sub>4</sub>	Pb(II)	23.6	-
	Zn(II)	12	19.0
	Cu(II)	16	15.0
	Co(II)	23	10.3
PAN/ <i>M. oleifera</i> /Fe <sub>3</sub> O <sub>4</sub> :Co	Pb(II)	32.0	-
	Zn(II)	17	18.8
	Cu(II)	19	17.2
	Co(II)	29	11.0
PAN/ <i>M. oleifera</i> /Fe <sub>3</sub> O <sub>4</sub> :Mn	Pb(II)	50.1	-
	Zn(II)	17	30.4
	Cu(II)	17	30.2
	Co(II)	19	30.4

**Fig. 4** Adsorption capacity during five adsorption–desorption cycles

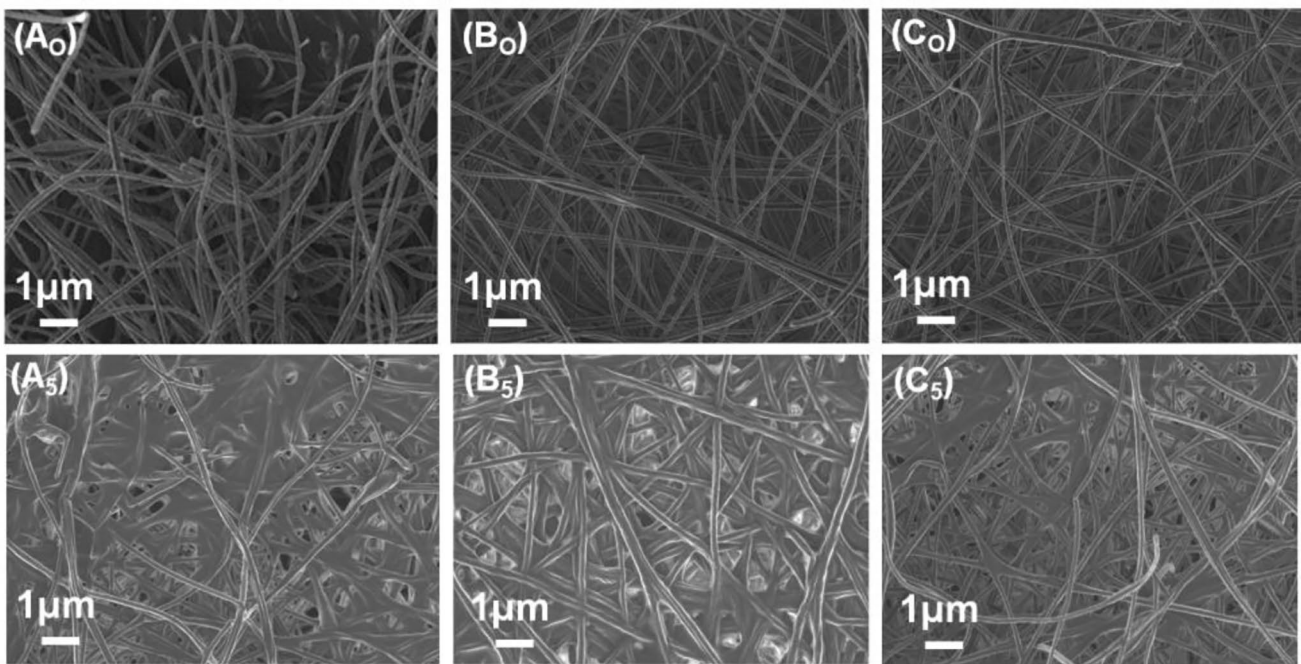
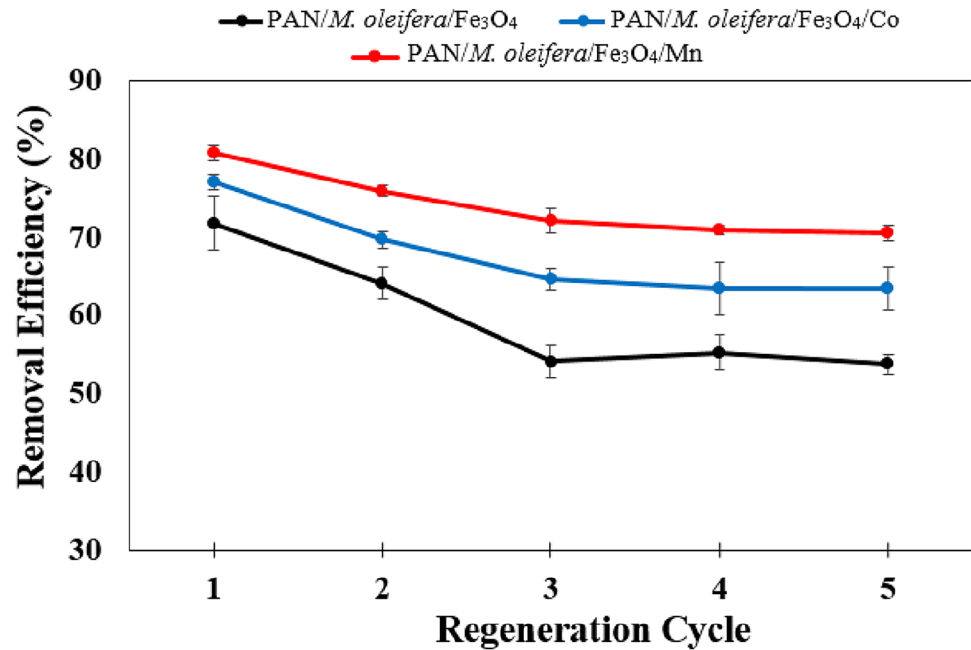


**Fig. 5** Morphology of **A<sub>0</sub>** PAN/*M. oleifera*/Fe<sub>3</sub>O<sub>4</sub> before and **A<sub>5</sub>** after adsorption cycles **B<sub>0</sub>** PAN/*M. oleifera*/Fe<sub>3</sub>O<sub>4</sub>/Co before and **B<sub>5</sub>** after adsorption cycles **C<sub>0</sub>** PAN/*M. oleifera*/Fe<sub>3</sub>O<sub>4</sub>/Mn before **C<sub>5</sub>** after adsorption cycles

desorption capability and effectiveness in regenerating adsorbents [76, 77]. To address disposal challenges, the implementation of acid recovery systems to recycle and reuse HNO<sub>3</sub> in multiple desorption cycles can assist in minimizing the environmental impact of nitric acid usage while maintaining the effectiveness of the adsorption–desorption process. More recently, there have been advances in the potential of using micro-wave-assisted, electrochemical and ultrasound regeneration techniques for desorption [76].

### 3.6 Economic assessment

To estimate the viable use of these adsorbents, a basic cost evaluation was performed with the main focus on primary expenses such as materials and energy. In determining the operating cost (OC), Eq. (5) was used:

$$OC \left( \frac{\text{USD}}{\text{m}^3} \right) = aC_{\text{energy}} + bC_{\text{chemicals}} \quad (5)$$

where  $C_{\text{energy}}$  is the energy consumed (in kWh/m<sup>3</sup>),

$C_{\text{chemicals}}$  is the chemical consumption (in kg/m<sup>3</sup>),

$a$  is the electrical energy price (USD 0.112/kWh) [78], and.

$b$  is the price of the chemicals used in the preparation (USD/kg or USD/m<sup>3</sup>).

In this study, the synthesized material could treat 0.030 L of wastewater in the first cycle; however, the calculated operating cost was done on a basis of treating 1 m<sup>3</sup> of the synthesized aqueous solution [79]. The study considered the power rating in watt for all the equipment used and the duration for which it was operated as well as the cost of the chemicals. Therefore, the total energy consumption was 105.0 kWh/m<sup>3</sup>, which equate to USD 12.47/m<sup>3</sup>, and total chemical cost was USD 2.06/m<sup>3</sup>. The operating cost was calculated to be USD 14.53 and compares well to other studies of a similar nature [18]. Regions in which energy costs are lower or alternative greener energy solutions are available, would make the use of these composite fibres aa attractive alternative.

## 4 Conclusion

Nanofibers, with their high surface area, tunable porosity, and functional versatility, are emerging as a promising solution for water remediation. This study demonstrates the adsorption efficiency, selectivity, and durability of electrospun composite nanofibers synthesized from *M. oleifera* seed biomass, MONPs and PAN polymer blend. The composite nanofibers (PAN/*M. oleifera*/Fe<sub>3</sub>O<sub>4</sub>, PAN/*M. oleifera*/Fe<sub>3</sub>O<sub>4</sub>:Co, and PAN/*M. oleifera*/Fe<sub>3</sub>O<sub>4</sub>:Mn) exhibited strong affinity for Pb(II) adsorption, with removal efficiencies ranging from 71.7% to 80.7% in naturally contaminated wastewater. Despite the presence of competing cations, the nanofibers maintained a high selectivity (K) towards Pb(II), with values between 10.3 and 30.4, indicating their preferential adsorption capability. Furthermore, the composite nanofibers demonstrated remarkable stability over multiple adsorption–desorption cycles, with only a 13% reduction in adsorption capacity after five cycles for PAN/*M. oleifera*/Fe<sub>3</sub>O<sub>4</sub>:Mn—the most effective composite. The cost assessment of this nanofiber adsorbent highlights its economic viability, positioning it as a competitive alternative to conventional adsorbents like activated carbon and biochar. These findings suggest that the developed adsorbents hold significant potential for addressing heavy metal contamination in wastewater through an environmentally sustainable and cost-effective approach. However, further optimization for large-scale production and field application is necessary to fully realize their potential in practical water treatment applications.

**Acknowledgements** RN is grateful for the scholarship from the German Academic Exchange Service scholarship (DAAD). We are grateful to Dr. Musyoka, Dr. Bambilaza, and Mrs. Mehlo from the Council for Scientific and Industrial Research (CSIR) and Prof. M. J. Moloto for use of the electrospinning equipment.

**Author contributions** N.N. and L.P. contributed to the study conception and design. Material preparation, data collection and analysis were performed by R.N., N.N. and L.P.. The first draft of the manuscript was written by R.N. and finalised by L.P.. All authors commented on subsequent versions of the manuscript. All authors read and approved the final manuscript.

**Funding** This work was supported by the University of Pretoria and National Research Foundation (TTK14051367221).

**Data availability** The data sets generated are available from the corresponding author upon request.

## Declarations

**Ethical approval and consent to participate** Not applicable.

**Consent to publication** Not applicable.

**Competing interests** The authors declare no competing interests.

**Open Access** This article is licensed under a Creative Commons Attribution-NonCommercial-NoDerivatives 4.0 International License, which permits any non-commercial use, sharing, distribution and reproduction in any medium or format, as long as you give appropriate credit to the original author(s) and the source, provide a link to the Creative Commons licence, and indicate if you modified the licensed material. You do not have permission under this licence to share adapted material derived from this article or parts of it. The images or other third party material in this article are included in the article's Creative Commons licence, unless indicated otherwise in a credit line to the material. If material is not included in the article's Creative Commons licence and your intended use is not permitted by statutory regulation or exceeds the permitted use, you will need to obtain permission directly from the copyright holder. To view a copy of this licence, visit <http://creativecommons.org/licenses/by-nc-nd/4.0/>.

## References

1. Chakraborty R, Asthana A, Singh AK, Jain B, Susan ABH. Adsorption of Heavy Metal Ions by Various Low-Cost Adsorbents: A Review. *Int J Environ Anal Chem.* 2022;102(2):342–79. <https://doi.org/10.1080/03067319.2020.1722811>.
2. Edo GI, Samuel PO, Oloni GO, Ezekiel GO, Ikpekoru VO, Obasohan P, Ongulu J, Otunuya CF, Opiti AR, Ajakaye RS, Essaghah AEA, Agbo JJ. Environmental Persistence, Bioaccumulation, and Ecotoxicology of Heavy Metals. *Chem Ecol.* 2024;40(3):322–49. <https://doi.org/10.1080/02757540.2024.2306839>.
3. Feng X, Long R, Wang L, Liu C, Bai Z, Liu X. A Review on Heavy Metal Ions Adsorption from Water by Layered Double Hydroxide and Its Composites. *Sep Purif Technol.* 2022;284: 120099. <https://doi.org/10.1016/j.seppur.2021.120099>.
4. Moukadiri H, Noukrati H, Ben Youcef H, Iraola I, Trabadelo V, Ouarrour A, Malka G, Barroug A. Impact and Toxicity of Heavy Metals on Human Health and Latest Trends in Removal Process from Aquatic Media. *Int J Environ Sci Technol.* 2024;21(3):3407–44. <https://doi.org/10.1007/s13762-023-05275-z>.
5. Sharma, A.; Grewal, A. S.; Sharma, D.; Srivastav, A. L. Chapter 3 - Heavy Metal Contamination in Water: Consequences on Human Health and Environment. In *Metals in Water*; Shukla, S. K., Kumar, S., Madhav, S., Mishra, P. K., Eds.; Advances in Environmental Pollution Research; Elsevier, 2023; pp 39–52. <https://doi.org/10.1016/B978-0-323-95919-3.00015-X>.
6. Aransiola SA, Josiah IUJ, Abioye OP, Bala JD, Rivadeneira-Mendoza BF, Prasad R, Luque R, Rodríguez-Díaz JM, Maddela NR. Micro and Vermicompost Assisted Remediation of Heavy Metal Contaminated Soils Using Phytoextractors. *Case Stud Chem Environ Eng.* 2024;9: 100755. <https://doi.org/10.1016/j.csee.2024.100755>.
7. Arora NK, Chauhan R. Heavy Metal Toxicity and Sustainable Interventions for Their Decontamination. *Environ Sustain.* 2021;4(1):1–3. <https://doi.org/10.1007/s42398-021-00164-y>.
8. Diaconu M, Pavel LV, Hlihor R-M, Rosca M, Fertu DI, Lenz M, Corvini PX, Gavrilescu M. Characterization of Heavy Metal Toxicity in Some Plants and Microorganisms—A Preliminary Approach for Environmental Bioremediation. *New Biotechnol.* 2020;56:130–9. <https://doi.org/10.1016/j.nbt.2020.01.003>.
9. Xia F, Zhao Z, Niu X, Wang Z. Integrated Pollution Analysis, Pollution Area Identification and Source Apportionment of Heavy Metal Contamination in Agricultural Soil. *J Hazard Mater.* 2024;465: 133215. <https://doi.org/10.1016/j.jhazmat.2023.133215>.
10. Saravanan A, Kumar PS, Jeevanantham S, Karishma S, Tajsabreen B, Yaashikaa PR, Reshma B. Effective Water/Wastewater Treatment Methodologies for Toxic Pollutants Removal: Processes and Applications towards Sustainable Development. *Chemosphere.* 2021;280: 130595. <https://doi.org/10.1016/j.chemosphere.2021.130595>.
11. Ovuoraye PE, Ugonabo VI, Enyoh CE, Igwegbe CA, Egbosiuba TC, Ibrahim I. Exploring Mechanistic Insights Into Coagulation-Flocculation-Aided Adsorption Design: A Comprehensive Study On the Removal of Toxic Metals and Organic Pollutants From Vegetable Oil Processing Wastewater. *Environ Monit Assess.* 2025;197(3):304. <https://doi.org/10.1007/s10661-025-13732-0>.
12. Tong J, Chang B, Liu Y, Li B, Zhang Y, Han L, Wang J, Hu K, Shi K, Yang J. Efficient Capture of ReO<sub>4</sub><sup>-</sup>/TcO<sub>4</sub><sup>-</sup> on Anion Exchange Resin from Wastewater. *Sep Purif Technol.* 2025;352: 128168. <https://doi.org/10.1016/j.seppur.2024.128168>.
13. Pujari M, Shingan B, Arya AK, Naga Chaitanya G. Review on Synthesis of Ceramic Membranes to Mitigate Membrane Fouling in Oil-Water Separation. *Chem Eng Technol.* 2025;48(2): e202400273. <https://doi.org/10.1002/ceat.202400273>.
14. Aryanti PTP, Nugroho FA, Phalakornkule C, Kadier A. Energy Efficiency in Electrocoagulation Processes for Sustainable Water and Wastewater Treatment. *J Environ Chem Eng.* 2024;12(6): 114124. <https://doi.org/10.1016/j.jece.2024.114124>.
15. Buonomena MG, Mousavi SM, Hashemi SA, Lai CW. Water Cleaning Adsorptive Membranes for Efficient Removal of Heavy Metals and Metalloids. *Water.* 2022. <https://doi.org/10.3390/w14172718>.
16. Al-Gethami W, Qamar MA, Shariq M, Alaghaz A-NMA, Farhan A, Areshi AA, Alnasir MH. Emerging Environmentally Friendly Bio-Based Nanocomposites for the Efficient Removal of Dyes and Micropollutants from Wastewater by Adsorption: A Comprehensive Review. *RSC Adv.* 2024;14(4):2804–34. <https://doi.org/10.1039/D3RA06501D>.
17. Mosaffa E, Patel D, Ramsheh NA, Patel RI, Banerjee A, Ghafuri H. Bacterial Cellulose Microfiber Reinforced Hollow Chitosan Beads Decorated with Cross-Linked Melamine Plates for the Removal of the Congo Red. *Int J Biol Macromol.* 2024;254: 127794. <https://doi.org/10.1016/j.ijbiomac.2023.127794>.
18. Manamela L, Nombona N. Cellulose Acetate Supported MOF-5/Crystalline Nanocellulose Composite Film as an Adsorbent Material for Methylene Blue Removal from Aqueous Solutions. *ACS Omega.* 2024;9:37621–35.
19. Irma M, Foo KY, Susilawati S, Yusof ENM, Nishiyama N, Sabar S. Advancements in Zeolite and Zeolite-Based Sorbents: Modification Strategies in Mitigating Nitrogen-Containing Pollutants from Water and Wastewater. *Inorg Chem Commun.* 2025;172: 113715. <https://doi.org/10.1016/j.inoche.2024.113715>.
20. Xie S, Huang L, Su C, Yan J, Chen Z, Li M, Du M, Zhang H. Application of Clay Minerals as Adsorbents for Removing Heavy Metals from the Environment. *Green Smart Min Eng.* 2024;1(3):249–61. <https://doi.org/10.1016/j.gsm.2024.07.002>.

21. Sharma G, Verma A, Wang T, Naushad M, Kumar A, Dhiman P. Remediation of Antibiotics Using Coordination Polymers. *Coord Chem Rev.* 2024;519: 216120. <https://doi.org/10.1016/j.ccr.2024.216120>.
22. Alkhalidi H, Alharthi S, Alharthi S, AlGhamdi HA, AlZahrani YM, Mahmoud SA, Amin LG, Al-Shaalan NH, Boraie WE, Attia MS, Al-Gahtany SA, Aldaleeli N, Ghobashy MM, Sharshir AI, Madani M, Darwesh R, Abaza SF. Sustainable Polymeric Adsorbents for Adsorption-Based Water Remediation and Pathogen Deactivation: A Review. *RSC Adv.* 2024;14(45):33143–90. <https://doi.org/10.1039/D4RA05269B>.
23. Gunawardene OHP, Gunathilake CA, Vikrant K, Amaraweera SM. Carbon Dioxide Capture through Physical and Chemical Adsorption Using Porous Carbon Materials: A Review. *Atmosphere.* 2022. <https://doi.org/10.3390/atmos13030397>.
24. Khademian E, Salehi E, Sanaeepur H, Galiano F, Figoli A. A Systematic Review on Carbohydrate Biopolymers for Adsorptive Remediation of Copper Ions from Aqueous Environments-Part A: Classification and Modification Strategies. *Sci Total Environ.* 2020;738: 139829. <https://doi.org/10.1016/j.scitotenv.2020.139829>.
25. Manjubaashini N, Bargavi P, Balakumar S. Carbon Quantum Dots Derived from Agro Waste Biomass for Pioneering Bioanalysis and in Vivo Bioimaging. *J Photochem Photobiol Chem.* 2024;454: 115702. <https://doi.org/10.1016/j.jphotochem.2024.115702>.
26. Raza ZA, Munim SA, Ayub A. Recent Developments in Polysaccharide-Based Electrospun Nanofibers for Environmental Applications. *Carbohydr Res.* 2021;510: 108443. <https://doi.org/10.1016/j.carres.2021.108443>.
27. Sui F, Xue Z, Shao K, Hao Z, Ge H, Cui L, Quan G, Yan J. Iron-Modified Biochar Inhibiting Cd Uptake in Rice by Cd Co-Deposition with Fe Oxides in the Rice Rhizosphere. *Environ Sci Pollut Res.* 2024;31(17):26099–111. <https://doi.org/10.1007/s11356-024-32839-4>.
28. Pervez MdN, Stylios G. Investigating the Synthesis and Characterization of a Novel “Green” H<sub>2</sub>O<sub>2</sub>-Assisted, Water-Soluble Chitosan/Polyvinyl Alcohol Nanofiber for Environmental End Uses. *Nanomaterials.* 2018;8:395. <https://doi.org/10.3390/nano8060395>.
29. Talukder ME, Pervez MN, Jianming W, Gao Z, Stylios GK, Hassan MM, Song H, Naddeo V. Chitosan-Functionalized Sodium Alginate-Based Electrospun Nanofiber Membrane for As (III) Removal from Aqueous Solution. *J Environ Chem Eng.* 2021;9(6): 106693. <https://doi.org/10.1016/j.jece.2021.106693>.
30. Talukder ME, Pervez MdN, Jianming W, Stylios GK, Hassan MM, Song H, Naddeo V, Figoli A. Ag Nanoparticles Immobilized Sulfonated Polyethersulfone/Polyethersulfone Electrospun Nanofiber Membrane for the Removal of Heavy Metals. *Sci Rep.* 2022;12(1):5814. <https://doi.org/10.1038/s41598-022-09802-9>.
31. Wu P, Wang Y, Liu Y. Recent Advances in Heteroatom-Doped Porous Carbon for Adsorption of Gaseous Pollutants. *Chem Eng J.* 2024;491: 152142. <https://doi.org/10.1016/j.cej.2024.152142>.
32. Slezak R, Krzystek L, Puchalski M, Krucińska I, Sitariski A. Degradation of Bio-Based Film Plastics in Soil under Natural Conditions. *Sci Total Environ.* 2023;866: 161401. <https://doi.org/10.1016/j.scitotenv.2023.161401>.
33. Rostami MS, Khodaei MM. Recent Advances in Chitosan-Based Nanocomposites for Adsorption and Removal of Heavy Metal Ions. *Int J Biol Macromol.* 2024;270: 132386. <https://doi.org/10.1016/j.ijbiomac.2024.132386>.
34. Khalid AM, Hossain MdS, Khalil NA, Zulkifli M, Arafath MdA, Shaharun MS, Ayub R, Ahmad Yahaya AN, Ismail N. Adsorptive Elimination of Heavy Metals from Aqueous Solution Using Magnetic Chitosan/Cellulose-Fe(III) Composite as a Bio-Sorbent. *Nanomaterials.* 2023. <https://doi.org/10.3390/nano13101595>.
35. Peng S, Meng H, Ouyang Y, Chang J. Nanoporous Magnetic Cellulose-Chitosan Composite Microspheres: Preparation, Characterization, and Application for Cu(II) Adsorption. *Ind Eng Chem Res.* 2014;53(6):2106–13. <https://doi.org/10.1021/ie402855t>.
36. Araújo LCC, Aguiar JS, Napoleão TH, Mota FVB, Barros ALS, Moura MC, Coriolano MC, Coelho LCBB, Silva TG, Paiva PMG. Evaluation of Cytotoxic and Anti-Inflammatory Activities of Extracts and Lectins from Moringa Oleifera Seeds. *PLoS ONE.* 2013;8(12): e81973. <https://doi.org/10.1371/journal.pone.0081973>.
37. Ngulube R, Pillay L, Nombona N. Synthesis and Characterization of Electrospun Composite Nanofibers from Moringa Oleifera Biomass and Metal Oxide Nanoparticles as Potential Adsorbents for the Removal of Lead Ions. *Chem Pap.* 2023. <https://doi.org/10.1007/s11696-023-03115-5>.
38. Thamer BM, Aldalbahi A, Moydeen A, M., Rahaman, M., El-Newehy, M. H. Modified Electrospun Polymeric Nanofibers and Their Nanocomposites as Nanoadsorbents for Toxic Dye Removal from Contaminated Waters: A Review. *Polymers.* 2021. <https://doi.org/10.3390/polym13010020>.
39. Sengul AB, Asmatulu E. Toxicity of Metal and Metal Oxide Nanoparticles: A Review. *Environ Chem Lett.* 2020;18(5):1659–83. <https://doi.org/10.1007/s10311-020-01033-6>.
40. Mascolo MC, Pei Y, Ring TA. Room Temperature Co-Precipitation Synthesis of Magnetite Nanoparticles in a Large pH Window with Different Bases. *Materials.* 2013;6(12):5549–67. <https://doi.org/10.3390/ma6125549>.
41. Wahab A, Imran M, Ikram M, Naz M, Aqeel M, Rafiq A, Majeed H, Ali S. Dye Degradation Property of Cobalt and Manganese Doped Iron Oxide Nanoparticles. *Appl Nanosci.* 2019;9(8):1823–32. <https://doi.org/10.1007/s13204-019-00970-1>.
42. Warner CL, Chouyyok W, Mackie KE, Neiner D, Saraf LV, Droubay TC, Warner MG, Addleman RS. Manganese Doping of Magnetic Iron Oxide Nanoparticles: Tailoring Surface Reactivity for a Regenerable Heavy Metal Sorbent. *Langmuir.* 2012;28(8):3931–7. <https://doi.org/10.1021/la2042235>.
43. dos Santos TRT, Bongiovani MC, Silva MF, Nishi L, Coldebella PF, Vieira MF, Bergamasco R. Trihalomethanes Minimization in Drinking Water by Coagulation/Flocculation/Sedimentation with Natural Coagulant Moringa Oleifera Lam and Activated Carbon Filtration. *Can J Chem Eng.* 2016;94(7):1277–84. <https://doi.org/10.1002/cjce.22506>.
44. Xiao Y, Helal AS, Mazarío E, Mayorál A, Chevillot-Biraud A, Decorse P, Losno R, Maurel F, Ammar S, Lomas JS, Hémadi M. Functionalized Maghemite Nanoparticles for Enhanced Adsorption of Uranium from Simulated Wastewater and Magnetic Harvesting. *Environ Res.* 2023;216: 114569. <https://doi.org/10.1016/j.envres.2022.114569>.
45. Kříbek B, Nyambe I, Majer V, Knésl I, Mihaljevič M, Ettlér V, Vaněk A, Penížek V, Sracek O. Soil Contamination near the Kabwe Pb-Zn Smelter in Zambia: Environmental Impacts and Remediation Measures Proposal. *J Geochem Explor.* 2019;197:159–73. <https://doi.org/10.1016/j.gexplo.2018.11.018>.
46. Leteinturier B, Laroche J, Matera J, Malaisse F. Reclamation of Lead / Zinc Processing Wastes at Kabwe, Zambia : A Phytogeochemical Approach. *South Afr J Sci.* 2001;97(11):624–7. <https://doi.org/10.10520/EJC97230>.

47. Moonga G, Chisola MN, Berger U, Nowak D, Yabe J, Nakata H, Nakayama S, Ishizuka M, Bose-O'Reilly S. Geospatial Approach to Investigate Spatial Clustering and Hotspots of Blood Lead Levels in Children within Kabwe. *Zambia Environ Res.* 2022;207:112646. <https://doi.org/10.1016/j.envres.2021.112646>.
48. Yamada D, Hiwatari M, Narita D, Hangoma P, Chitah B, Nakata H, Nakayama SMM, Yabe J, Ito M, Igarashi T, Ishizuka M, Zyambo G. Social Cost of Mining-Related Lead (Pb) Pollution in Kabwe, Zambia, and Potential Remediation Measures. *Sci Total Environ.* 2023;865:161281. <https://doi.org/10.1016/j.scitotenv.2022.161281>.
49. Mufalo W, Arima T, Igarashi T, Ito M, Sato T, Tomiyama S, Nyambe I, Tabelin CB, Nakata H, Nakayama S, Ishizuka M. Insights on Hazardous Metal Bioaccessibility, and Groundwater Impacted by Zn Residues from a Legacy Mine and Risk Evaluation of Adjacent Soils. *Environ Geochem Health.* 2024;46(2):64. <https://doi.org/10.1007/s10653-024-01864-0>.
50. Yabe J, Nakayama SMM, Ikenaka Y, Yohannes YB, Bortey-Sam N, Kabalo AN, Ntapisha J, Mizukawa H, Umemura T, Ishizuka M. Lead and Cadmium Excretion in Feces and Urine of Children from Polluted Townships near a Lead-Zinc Mine in Kabwe. *Zambia Chemosphere.* 2018;202:48–55. <https://doi.org/10.1016/j.chemosphere.2018.03.079>.
51. Araújo CST, Alves VN, Rezende HC, Almeida ILS, de Assunção RMN, Tarley CRT, Segatelli MG, Coelho NMM. Characterization and Use of Moringa Oleifera Seeds as Biosorbent for Removing Metal Ions from Aqueous Effluents. *Water Sci Technol.* 2010;62(9):2198–203. <https://doi.org/10.2166/wst.2010.419>.
52. Shariful MI, Sharif SB, Lee JLL, Habiba U, Ang BC, Amalina MA. Adsorption of Divalent Heavy Metal Ion by Mesoporous-High Surface Area Chitosan/Poly (Ethylene Oxide) Nanofibrous Membrane. *Carbohydr Polym.* 2017;157:57–64. <https://doi.org/10.1016/j.carbpol.2016.09.063>.
53. Bhutada PR, Jadhav AJ, Pinjari DV, Nemade PR, Jain RD. Solvent Assisted Extraction of Oil from Moringa Oleifera Lam. Seeds Ind Crops Prod. 2016;82:74–80. <https://doi.org/10.1016/j.indcrop.2015.12.004>.
54. Ibrahim NA, Bibi S, Khan AK, G. M. Development and Butyrylcholinesterase/Monoamine Oxidase Inhibition Potential of PVA-Moringa Oleifera Developed Nanofibers. *J Exp Nanosci.* 2022;17(1):34–46. <https://doi.org/10.1080/17458080.2021.2016712>.
55. Fayemi OE, Ekennia AC, Katata-Seru L, Ebokaiwe AP, Ijomone OM, Onwudiwe DC, Ebenso EE. Antimicrobial and Wound Healing Properties of Polyacrylonitrile-Moringa Extract Nanofibers. *ACS Omega.* 2018;3(5):4791–7. <https://doi.org/10.1021/acsomega.7b01981>.
56. Narayan M, Sadasivam R, Packirisamy G, Pichiah S. Electrospun Polyacrylonitrile-Moringa Oleifera Based Nanofibrous Bio-Sorbent for Remediation of Congo Red Dye. *J Environ Manage.* 2022;317:115294. <https://doi.org/10.1016/j.jenvman.2022.115294>.
57. Ye Y, Cota-Ruiz K, Hernández-Viezcás JA, Valdés C, Medina-Velo IA, Turley RS, Peralta-Videa JR, Gardea-Torresdey JL. Manganese Nanoparticles Control Salinity-Modulated Molecular Responses in Capsicum Annuum L. through Priming: A Sustainable Approach for Agriculture. *ACS Sustain Chem Eng.* 2020;8(3):1427–36. <https://doi.org/10.1021/acssuschemeng.9b05615>.
58. Cai Y, Fang M, Tan X, Hu B, Wang X. Highly Efficient Selective Elimination of Heavy Metals from Solutions by Different Strategies. *Sep Purif Technol.* 2024;350:127975. <https://doi.org/10.1016/j.seppur.2024.127975>.
59. Wang S, Hu J, Li J, Dong Y. Influence of pH, Soil Humic/Fulvic Acid, Ionic Strength, Foreign Ions and Addition Sequences on Adsorption of Pb(II) onto GMZ Bentonite. *J Hazard Mater.* 2009;167(1):44–51. <https://doi.org/10.1016/j.jhazmat.2008.12.079>.
60. Gao C, Wang X-L, An Q-D, Xiao Z-Y, Zhai S-R. Synergistic Preparation of Modified Alginate Aerogel with Melamine/Chitosan for Efficiently Selective Adsorption of Lead Ions. *Carbohydr Polym.* 2021;256:117564. <https://doi.org/10.1016/j.carbpol.2020.117564>.
61. Bakhtari S, Salari M, Shahrashoub M, Zeidabadinejad A, Sharma G, Sillanpää M. A Comprehensive Review on Green and Eco-Friendly Nano-Adsorbents for the Removal of Heavy Metal Ions: Synthesis, Adsorption Mechanisms, and Applications. *Curr Pollut Rep.* 2024;10(1):1–39. <https://doi.org/10.1007/s40726-023-00290-7>.
62. Bo S, Luo J, An Q, Xiao Z, Wang H, Cai W, Zhai S, Li Z. Efficiently Selective Adsorption of Pb(II) with Functionalized Alginate-Based Adsorbent in Batch/Column Systems: Mechanism and Application Simulation. *J Clean Prod.* 2020;250:119585. <https://doi.org/10.1016/j.jclepro.2019.119585>.
63. Chander S, Yadav S, Sharma HR, Gupta A. Sequestration of Cd (II) Utilizing Biowaste-Fabricated Recyclable Mesoporous Magnetite (Fe<sub>3</sub>O<sub>4</sub>) Nano-Adsorbent: Process Optimization, Thermodynamic Investigation, Simulation Modeling, and Feasibility for Electroplating Effluent. *J Alloys Compd.* 2024;986:174088. <https://doi.org/10.1016/j.jallcom.2024.174088>.
64. Osińska M. Removal of Lead(II), Copper(II), Cobalt(II) and Nickel(II) Ions from Aqueous Solutions Using Carbon Gels. *J Sol-Gel Sci Technol.* 2017;81(3):678–92. <https://doi.org/10.1007/s10971-016-4256-0>.
65. Habib S, Akoumeh R, Mahdi E, Al-Ejji M, Hassan MK, Hawari AH. A Facile One-Step Sustainable Synthesis of Magnetic Hyperbranched Dendritic Polyester HBPE for Efficient Trace Removal of Lead and Copper Ions. *J Water Process Eng.* 2024;60:105280. <https://doi.org/10.1016/j.jwpe.2024.105280>.
66. Moyo A, Parbhakar-Fox A, Meffre S, Cooke DR. Alkaline Industrial Wastes – Characteristics, Environmental Risks, and Potential for Mine Waste Management. *Environ Pollut.* 2023;323:121292. <https://doi.org/10.1016/j.envpol.2023.121292>.
67. Patel PK, Pandey LM, Uppaluri RVS. Adsorptive Removal of Zn, Fe, and Pb from Zn Dominant Simulated Industrial Wastewater Solution Using Polyvinyl Alcohol Grafted Chitosan Variant Resins. *Chem Eng J.* 2023;459:141563. <https://doi.org/10.1016/j.cej.2023.141563>.
68. Sopanrao KS, Sreedhar I. Polyvinyl Alcohol Modified Chitosan Composite as a Novel and Efficient Adsorbent for Multi-Metal Removal. *Sep Purif Technol.* 2024;340:126731. <https://doi.org/10.1016/j.seppur.2024.126731>.
69. Song X, Nong L, Zhang M, Liu J. Efficient Removal of As (III) by a La/Fe Composite Membrane Filter: The Composite Form of La, the Dynamic Adsorption and Adaptability. *J Environ Chem Eng.* 2024;12(4):113056. <https://doi.org/10.1016/j.jece.2024.113056>.
70. Kinraide TB, Yermiyahu U. A Scale of Metal Ion Binding Strengths Correlating with Ionic Charge, Pauling Electronegativity, Toxicity, and Other Physiological Effects. *J Inorg Biochem.* 2007;101(9):1201–13. <https://doi.org/10.1016/j.jinorgbio.2007.06.003>.
71. Panayotova M, Velikov B. Influence of Zeolite Transformation in a Homoionic Form on the Removal of Some Heavy Metal Ions from Wastewater. *J Environ Sci Health Part A Tox Hazard Subst Environ Eng.* 2003;38(545):554. <https://doi.org/10.1081/ESE-120016916>.
72. Zhu F, Zheng Y-M, Zhang B-G, Dai Y-R. A Critical Review on the Electrospun Nanofibrous Membranes for the Adsorption of Heavy Metals in Water Treatment. *J Hazard Mater.* 2021;401:123608. <https://doi.org/10.1016/j.jhazmat.2020.123608>.
73. Seredych M, Bandoz TJ. Mechanism of Ammonia Retention on Graphite Oxides: Role of Surface Chemistry and Structure. *J Phys Chem C.* 2007;111(43):15596–604. <https://doi.org/10.1021/jp0735785>.

74. Xie W, Shi Y, Wang Y, Zheng Y, Liu H, Hu Q, Wei S, Gu H, Guo Z. Electrospun Iron/Cobalt Alloy Nanoparticles on Carbon Nanofibers towards Exhaustive Electrocatalytic Degradation of Tetracycline in Wastewater. *Chem Eng J.* 2021;405: 126585. <https://doi.org/10.1016/j.cej.2020.126585>.
75. Pandey RK, Lakshminarayanan V. Electro-Oxidation of Formic Acid, Methanol, and Ethanol on Electrodeposited Pd-Polyaniline Nanofiber Films in Acidic and Alkaline Medium. *J Phys Chem C.* 2009;113(52):21596–603. <https://doi.org/10.1021/jp908239m>.
76. Leng Y, Xu J, Wei J, Ye G. Amino-Bearing Calixcrown Receptor Grafted to Micro-Sized Silica Particles for Highly Selective Enrichment of Palladium in HNO<sub>3</sub> Media. *Chem Eng J.* 2013;232:319–26. <https://doi.org/10.1016/j.cej.2013.07.116>.
77. Yuan D, Zhang S, Xiang Z, He Y, Wang Y, Liu Y, Zhao X, Zhou X, Zhang Q. Highly Efficient Removal of Thorium in Strong HNO<sub>3</sub> Media Using a Novel Polymer Adsorbent Bearing a Phosphonic Acid Ligand: A Combined Experimental and Density Functional Theory Study. *ACS Appl Mater Interfaces.* 2019;11(27):24512–22. <https://doi.org/10.1021/acsami.9b03674>.
78. Bekezulu, N. *Schedule of Standard Fees 2025/26*; 240–143103800; Eskom Holdings SOC Ltd, 2025; p 29.
79. Bayramoglu M, Kobyas M, Can OT, Sozbir M. Operating Cost Analysis of Electrocoagulation of Textile Dye Wastewater. *Sep Purif Technol.* 2004;37(2):117–25. <https://doi.org/10.1016/j.seppur.2003.09.002>.

**Publisher's Note** Springer Nature remains neutral with regard to jurisdictional claims in published maps and institutional affiliations.